J Supercond Nov Magn (2008) 21: 81–85
DOI 10.1007/s10948-007-0302-z

# *s*-Wave Symmetry Along the *c*-Axis and $s + d$ In-plane Superconductivity in Bulk $YBa_2Cu_4O_8$

**R. Khasanov · A. Shengelaya · J. Karpinski · A. Bussmann-Holder · H. Keller · K.A. Müller**

Received: 12 September 2007 / Accepted: 19 September 2007 / Published online: 20 December 2007


**Abstract** To clarify the order parameter symmetry of cuprates, the magnetic penetration depth $\lambda$ was measured along the crystallographic directions $a$, $b$, and $c$ in single crystals of $YBa_2Cu_4O_8$ via muon spin rotation. *This method is direct, bulk sensitive, and unambiguous*. The temperature dependences of $\lambda_a^{-2}$ and $\lambda_b^{-2}$ exhibit an inflection point at low temperatures as is typical for two-gap superconductivity (TGS) with $s + d$-wave character in the planes. Perpendicular to the planes a pure $s$-wave gap is observed thereby highlighting the important role of $c$-axis effects. We conclude that these are generic and universal features in the bulk of cuprates.

**PACS** 76.75.+i · 74.72.Bk · 74.25.Ha

Two gap superconductivity (TGS) remained a theoretical issue only for more than 20 years [1–3], even though it seemed to be a natural and intriguing extension of BCS theory for more complex materials. In 1980, TGS was finally observed in Nb doped $SrTiO_3$ [4] and believed to be a rare exception in superconductors. Since the discovery of TGS in $MgB_2$, many more superconductors with TGS were found, including heavy fermion compounds, making this feature more common than believed early on. In all of the above mentioned superconductors, the combined order parameters exhibit always the same symmetry, namely $s + s$ in Nb doped $SrTiO_3$ [4] and $MgB_2$ [5] and $d + d$ in heavy fermion compounds [6]. A totally novel situation is met in cuprate high-temperature superconductors (HTS), since the order parameters are of different symmetries, i.e., $s + d$ [7–13]. However, theoretical modeling suggested a single $d$-wave order parameter in the $CuO_2$ planes, and unfortunately biased further research and partly inhibited the experimental efforts to characterize TGS in more detail in HTS.

Recently, new muon spin rotation ($\mu$SR) investigations of single crystal $La_{1.83}Sr_{0.17}CuO_4$ detected an inflection point in the temperature dependence of the inverse-squared in-plane magnetic penetration depth $\lambda_{ab}^{-2}$, which is a direct consequence of two superconducting gaps with largely different zero temperature gap values [14]. Since it is unclear whether these observations are a material specific property or generic and intrinsic to HTS, the previous $\mu$SR studies were extended to single crystal $YBa_2Cu_4O_8$ and were performed by applying a magnetic field along the crystallographic directions $a$, $b$, and $c$. Thereby we obtain the three principle components of the second moments of the local magnetic field distribution $P(B)$ in the mixed state, which are related to the superfluid density, and reflect directly the corresponding penetration depths $\lambda_a$, $\lambda_b$, and $\lambda_c$. While $\lambda_a^{-2}$ and $\lambda_b^{-2}$ vary almost linearly with temperature for $20 < T < 50$ K, as is expected for a $d$-wave order parameter, the $c$-axis response ($\lambda_c^{-2}$) saturates below 30 K, as expected for a $s$-wave order parameter. In addition, $\lambda_a^{-2}$ and

R. Khasanov (✉) · H. Keller · K.A. Müller
Physik-Institut der Universität Zürich, Winterthurerstrasse 190, 8057 Zürich, Switzerland
e-mail: khasanov@physik.uzh.ch

A. Shengelaya
Physics Institute of Tbilisi State University, Chavchadze 3, 0128 Tbilisi, Georgia

J. Karpinski
Laboratory for Solid State Physics, ETH Zürich, 8093 Zürich, Switzerland

A. Bussmann-Holder
Max-Planck-Institut für Festkörperforschung, Heisenbergstrasse 1, 70569 Stuttgart, Germany

$\lambda_b^{-2}$, both exhibit an inflection point in their temperature dependences around $T \simeq 10$ K which—as has been shown in [15]—is the consequence of two coexisting order parameters, namely $s + d$.

Details of the sample preparation for $YBa_2Cu_4O_8$ can be found elsewhere [16]. All crystals used in the present study were taken from one batch. The superconducting transition temperature $T_c$ and the width of the superconducting transition $\Delta T_c$ were determined for the three sets ($\simeq$40–50 crystals each) of the main set ($\simeq$130) of crystals. Both were obtained from field-cooled (0.5 mT) magnetization curves measured by a SQUID magnetometer and exhibited all the same values, i.e., $T_c \simeq 79.9$ K and $\Delta T_c \simeq 2$ K. The crystals had mostly a rectangular shape with a typical size of approximately $0.8 \times 0.3 \times 0.05$ mm$^3$. X-ray measurements revealed that the crystallographic $b$-axis is exactly parallel to the longest side. Bearing in mind that the $c$-axis is perpendicular to the flat surface of the crystal, we were able to orient the whole set along the crystallographic $a$, $b$, and $c$ directions. The final orientation of the crystals in the mosaic was checked by using a polarizing microscope.

The transverse-field $\mu$SR experiments on a mosaic of oriented $YBa_2Cu_4O_8$ single crystals were done at the $\pi$M3 and $\pi$E1 beam lines at the Paul Scherrer Institute (Villigen, Switzerland). The mosaic was field cooled from above $T_c$ to 1.7 K in a field of 0.015 T. The $\mu$SR experiments were performed for the magnetic field applied parallel to the $a$, $b$, and $c$ crystallographic axes. Typical counting statistics were ~24–30 million muon detections over three detectors. In the analysis presented below, we used the well-known fact that for an extreme type-II superconductor in the mixed state $\lambda^{-4}$ is proportional to the second moment of the magnetic field distribution in the superconductor in the mixed state $P(B)$ probed by $\mu$SR [17]. The second moment of $P(B)$ was calculated within the same framework described in [14]. We used a four component Gaussian expression to fit the $\mu$SR time spectra. One component arises here from the background signal stemming from muons stopped outside the sample, whereas the other three components describe the asymmetric line shape of $P(B)$ in the mixed state (see inset to Fig. 1). The first and the second moments of $P(B)$ (excluding the background component) are then obtained as:

$$\langle B \rangle = \sum_{i=1}^{3} \frac{A_i B_i}{A_1 + A_2 + A_3} \tag{1}$$

and

$$\left\langle \Delta B^2 \right\rangle = \frac{\sigma^2}{\gamma_\mu^2} = \sum_{i=1}^{3} \frac{A_i}{A_1 + A_2 + A_3} \left[ \frac{\sigma_i^2}{\gamma_\mu^2} + \left[ B_i - \langle B \rangle \right]^2 \right]. \tag{2}$$

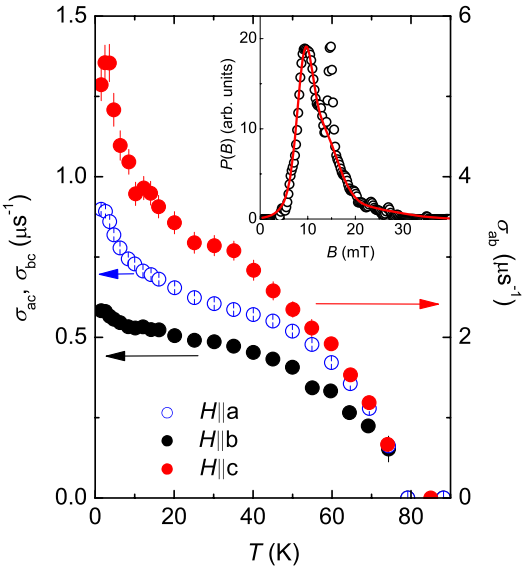


**Fig. 1** (Color online) Temperature dependences of $\sigma_{ab} \propto \lambda_{ab}^{-2}$ $(H \| c)$, $\sigma_{ac} \propto \lambda_{ac}^{-2}$ $(H \| b)$, and $\sigma_{bc} \propto \lambda_{bc}^{-2}$ $(H \| a)$ of $YBa_2Cu_4O_8$, measured after field cooling the sample in $\mu_0 H = 0.015$ T. The inset shows the local magnetic field distribution $P(B)$ obtained by means of the maximum entropy Fourier transform technique at $T = 1.7$ K and $\mu_0 H = 0.015$ T applied parallel to the $c$-axis (*open circles*: data; *solid line*: four component Gaussian fit excluding the background)

Here $\gamma_\mu = 2\pi \times 135.5342$ MHz/T is the muon gyromagnetic ratio. $A_i$, $\sigma_i$, and $B_i$ are the asymmetry, the relaxation rate, and the first moment of the $i$th component, respectively. The superconducting part of the square root of the second moment ($\sigma_{sc} \propto \lambda^{-2}$) was then obtained by subtracting the nuclear moment contribution ($\sigma_{nm}$) measured at $T > T_c$, according to $\sigma_{sc}^2 = \sigma^2 - \sigma_{nm}^2$. To ensure that the increase of the second moment of the measured $\mu$SR signal below $T_c$ is attributed entirely to the vortex lattice, zero-field $\mu$SR experiments were performed. No evidence for static magnetism in the $YBa_2Cu_4O_8$ mosaic sample down to 1.7 K was observed.

For an anisotropic London superconductor, the effective penetration depth for the magnetic field along the $i$th crystallographic axis is given by [18]:

$$\lambda_{jk}^{-2} = \frac{1}{\lambda_j \lambda_k} \propto \sigma_{jk}. \tag{3}$$

Here the index "sc" for the superconducting part of the square root of the second moment $\sigma_{sc}$ is omitted for simplicity. From (3), it is obvious that for the magnetic field applied along one of the principal axes $a$, $b$, and $c$, the components $\sigma_{bc} \propto \lambda_{bc}^{-2}$, $\sigma_{ac} \propto \lambda_{ac}^{-2}$, and $\sigma_{ab} \propto \lambda_{ab}^{-2}$ are measured. The temperature dependences of $\sigma_{bc}$, $\sigma_{ac}$, and $\sigma_{ab}$ after field-cooling the sample in $\mu_0 H = 0.015$ T are shown in Fig. 1. It is seen that at $T_{ip} \sim$ 10–20 K all measured $\sigma_{ij}(T)$ exhibit an inflection point. Below this point, $\sigma_{ab}$, $\sigma_{bc}$, and $\sigma_{ac}$ increase by approximately 70%, 35%, and 10%, respec-

tively. Note that a similar inflection point in $\lambda_{ab}^{-2}(T)$ was also observed in low-field magnetization (LFM) experiments on powder samples of $YBa_2Cu_4O_8$ [19]. However, in these experiments, the increase of $\lambda_{ab}^{-2}$ below $T_{ip}$ was much less pronounced than the one observed in the present study. This difference can be explained by the fact that LFM probes the penetration depth mainly near the surface, whereas $\mu$SR measures $\lambda$ in the *bulk*. In LFM experiments the magnetic field penetrates the sample only on a distance $\lambda$ from the surface of the sample (few hundred nanometers), thereby leaving the main part of the superconducting volume unaffected. In contrast, muons penetrate at much longer distances into the sample (few-tenths of a millimeter), thus probing $\lambda$ deeply inside the sample. It should be recalled that at the surface due to the symmetry breaking, the order parameter has pure $d$-wave character, whereas in the bulk $s + d$-wave symmetry is present [11]. This illustrates in a natural way the difference between the surface sensitive LFM and the bulk sensitive $\mu$SR experiments. In addition, it provides a logical explanation why surface sensitive experiments predominantly detect a $d$-wave gap.

From (3), the individual components of $\lambda$ along the $i$th crystallographic direction are obtained as:

$$\sigma_i = \frac{\sigma_{ij}\sigma_{ik}}{\sigma_{jk}} \propto \frac{1}{\lambda_i^2}. \tag{4}$$

Figure 2 shows the temperature dependences of $\sigma_a \propto \lambda_a^{-2}$, $\sigma_b \propto \lambda_b^{-2}$, and $\sigma_c \propto \lambda_c^{-2}$ as derived from the data presented in Fig. 1 by using (4). In the following, we discuss the temperature dependence of each particular component separately.

From Figs. 2(a) and (b), it is evident that both $\sigma_a \propto \lambda_a^{-2}$ and $\sigma_b \propto \lambda_b^{-2}$ increase almost linearly with decreasing temperature in the range $50 < T < 20$ K. Around $T_{ip} \simeq 10$ K, an inflection point is visible in the temperature dependence. Below this point, an unusual increase in both quantities appears: $\sigma_a$ increases by almost 20% (from 2.95 $\mu s^{-1}$ at $T = 10$ K to 3.5 $\mu s^{-1}$ at $T = 2.6$ K), and $\sigma_b$ by 60% (from 5.2 $\mu s^{-1}$ at $T = 10$ K to 8.3 $\mu s^{-1}$ at $T = 2.6$ K). As has been shown in Ref. [15], an inflection point in $\lambda^{-2}(T)$ suggests the presence of at least two superconducting gaps in $YBa_2Cu_4O_8$ with very different gap values, i.e., a large gap and a small one. The same behavior was observed recently in $La_{1.83}Sr_{0.17}CuO_4$ by $\mu$SR [14], as well as in other HTS using various techniques [9–13], supporting a two-gap behavior with the larger gap being of $d$-wave and the smaller one of $s$-wave symmetry. The above data were analyzed by assuming that an $s$-wave and a $d$-wave gap contribute to $\sigma$ according to:

$$\sigma(T) = \sigma^d(T) + \sigma^s(T), \tag{5}$$

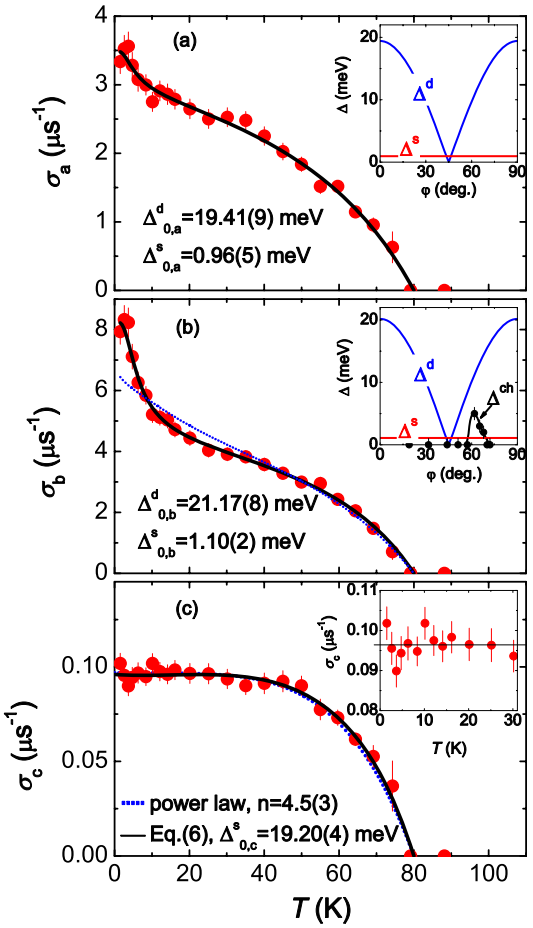


**Fig. 2** (Color online) Temperature dependences of $\sigma_a \propto \lambda_a^{-2}$ (**a**), $\sigma_b \propto \lambda_b^{-2}$ (**b**), and $\sigma_c \propto \lambda_c^{-2}$ (**c**) of $YBa_2Cu_4O_8$ at $\mu_0 H = 0.015$ T obtained from the data presented in Fig. 1 by means of (4). Lines in (**a**) and (**b**) represent results of the fits of $\sigma_a(T)$ and $\sigma_b(T)$ by means of the two-component (5) and the three-component models. The *blue dotted curve* in (**c**) represents a fit to the data assuming that $\sigma_b(T)$ is entirely determined by the in-plane $d$-wave and the chain gap measured in [20] (see text for details). The *black solid line* and the *blue dotted curve* in (**b**) represent fits by means of (6) with $g^s(\varphi) = 1$ and the power law $\sigma_c(T) = \sigma_c(0)[1 - (T/T_c)^n]$, respectively. The insets in (**a**) and (**b**) represent the angular dependences of the $d$-wave gap ($\Delta^d$), the $s$-wave gap ($\Delta^s$) and the gap in CuO chains ($\Delta^{ch}$) obtained in [20]. The inset in (**c**) shows $\sigma_c(T)$ at $T < 30$ K

where both components are expressed like [14]:

$$\frac{\sigma(T,\Delta_0)}{\sigma(0)} = 1 + \frac{1}{\pi}\int_0^{2\pi}\int_{\Delta(T,\varphi)}^{\infty}\left(\frac{\partial f}{\partial E}\right) \times \frac{E\,dE\,d\varphi}{\sqrt{E^2 - \Delta(T,\varphi)^2}}. \tag{6}$$

Here, $f = [1 + \exp(E/k_BT)]^{-1}$ is the Fermi function, $\Delta_0$ is the maximum value of the gap, and $\Delta(T,\varphi) = \Delta_0\tilde{\Delta}(T/T_c)g(\varphi)$. For the normalized gap $\tilde{\Delta}(T/T_c)$, tabulated values of Ref. [21] were used. The function $g(\varphi)$ describes the angular dependence of the gap and is given by

**Table 1** Summary of the gap analysis of the temperature dependences of $\sigma_i \propto \lambda_i^{-2}$ $(i = a, b, c)$ for $YBa_2Cu_4O_8$. The meaning of the parameters is explained in the text

| Component | $\Delta_{0,i}^{d}$ (meV) | $\Delta_{0,i}^{s}$ (meV) | $\gamma_{ab}^{\Delta^d}$ | $\gamma_{ab}^{\Delta^s}$ |
|---|---|---|---|---|
| $\sigma_a$ | 19.41(9) | 0.96(5) | – | – |
| $\sigma_b$ | 21.17(8) | 1.10(2) | 1.09(1) | 1.15(6) |
| $\sigma_c$ | – | 19.20(4) | – | – |

$g^d(\varphi) = |\cos(2\varphi)|$ for the $d$-wave gap [12] and $g^s(\varphi) = 1$ for the $s$-wave gap (see insets in Figs. 2(a) and (b)). From this analysis, we obtain $\Delta_{0,a}^{d} = 19.41(9)$ meV, $\sigma_a^d = 3.03(2)$ $\mu s^{-1}$, $\Delta_{0,a}^{s} = 0.96(5)$ meV, $\sigma_a^s = 0.48(2)$ $\mu s^{-1}$ and $\Delta_{0,b}^{d} = 21.17(8)$ meV, $\sigma_b^d = 4.66(2)$ $\mu s^{-1}$, $\Delta_{0,b}^{s} = 1.10(2)$ meV, $\sigma_b^s = 3.63(2)$ $\mu s^{-1}$ for $\sigma_a(T)$ and $\sigma_b(T)$, respectively. The main results are summarized in Table 1.

The temperature dependence of $\sigma_c \propto \lambda_c^{-2}$ differs significantly from the one of the in-plane components since it saturates at temperatures $T < 30K$ to become $T$ independent (see inset in Fig. 2(c)). This dependence is analyzed in two ways: (i) by using (6) with $g^s(\varphi) = 1$, yielding $\Delta_{0,c}^{s} = 19.20(4)$ meV, and (ii) by assuming the phenomenological power law $\sigma_c(T) = \sigma_c(0)[1 - (T/T_c)^n]$. The results are given in Table 1 and compared to the experimental data in Fig. 2(c), from which it is obvious that both approaches are almost undistinguishable. For the power law dependence, a critical exponent $n = 4.5(3)$ is derived which is close to the one obtained within a two-fluid model where $n = 4$, which applies to a strong coupling $s$-wave BCS superconductors [22]. Using a $d$-wave model for a clean superconductor, Ref. [23] predicts an exponent $n = 5$. Since the observed power law exponent lies between these two values, it could be argued that $d$-wave superconductivity could also be the cause of the temperature dependence of $\sigma_c \propto \lambda_c^{-2}$. However, this can be ruled out since the results of Ref. [23] do not apply to cuprate superconductors containing chains, like $YBa_2Cu_3O_{7-\delta}$ and $YBa_2Cu_4O_8$. We can thus safely conclude that the order parameter along the $c$-axis is isotropic $s$-wave. This conclusion is further supported by $c$-axis tunneling [24], bicristal twist Josephson junctions [25], optical pulsed probe [26], and optical reflectivity (see Fig. 4 in Ref. [27]) experiments, as well as theoretical considerations [28]. It is important to note that due to the reasons described above the saturation of $\lambda_c^{-2}(T)$ obtained here has not been observed in LFM experiments [19].

The anisotropy observed in $\sigma_a$ and $\sigma_b$ and their unconventional temperature dependences deserve further remarks. The temperature dependences of both quantities are characterized by an inflection point at $T_{ip} \simeq 10$ K evidencing that at least two superconducting gaps contribute to the superfluid density. However, along the crystallographic $b$-direction this is much more pronounced than along $a$, and the analysis of both data sets in terms of $s + d$ wave gaps using (5) reveals that along the $a$ direction the $s$-wave order parameter contributes 14%, whereas along the $b$ direction the $s$-wave contribution is 42%. This assignment is supported by photoemission experiments on $YBa_2Cu_3O_{6.993}$, where a 50% difference in the magnitude of the superconducting gaps was reported [29]. In addition, these data provide evidence that this anisotropy is not a consequence of the chain related electronic structure, but intrinsic to the $CuO_2$ planes. Other experiments, like angle resolved electron tunneling [30] and phase sensitive Josephson contacts [31], yield similar anisotropy ratios and conclude also that deviations from pure $d$-wave symmetry are intrinsic to the planes. On the contrary, from Raman scattering spectra [10, 32], it was assumed that the anisotropy in the spectra along $a$ and $b$ directions stems from the chain contribution, where, however, the anisotropy ratio was of similar order of magnitude as reported here. Similar conclusions are reached by far infrared spectroscopy [33] where the observed anisotropy in the London penetration depth was suggested to be a consequence of the chain contribution. This latter conclusion can be excluded from the present experiment because first the fit of (5) to $\sigma_b(T)$, including a chain gap as observed by ARPES [20] (black curve in the inset of Fig. 2(b)), leads to a rather poor agreement with the experimental data (blue dotted curve in Fig. 2(b)). Second, the observation of an inflection point in $\sigma_a(T)$ cannot be explained by a possible misalignment of the crystals in the mosaic. $\sigma_a^s(0) = 0.48$ $\mu s^{-1}$ would correspond to a situation when *all* the crystals in the mosaic are turned by $\pm 8°$, or $\simeq 30°$ FWHM if one assumes a triangular distribution of orientations with the maximum along the crystallographic $b$ axis. Therefore, the data presented in Fig. 2(b) were analyzed by assuming that $\sigma_b(T)$ is the sum of three components: $\sigma_b^d(T)$, $\sigma_b^s(T)$, and the contribution from the chains $\sigma_b^{ch}(T)$. These results are, however, undistinguishable from the $s + d$ analysis presented above. It is important to note that independent of a possible chain related energy gap, both procedures provide clear evidence that the in-plane superconducting order parameter consists of two components, a $d$-wave order parameter and an additional $s$-wave component where the relative contributions of both components are less important than the fact that a mixture of both exists. This has also been shown theoretically [15], since the coupling between both components is the important quantity which substantially enhances $T_c$.

The maximum values of the in-plane $d$-wave gap along the $a$ and $b$ directions are of similar order of magnitudes, i.e., $\Delta_{0,a}^{d} = 19.41(9)$ meV, $\Delta_{0,b}^{d} = 21.17(8)$ meV, and thus in a good agreement with $\Delta_0^d = 22$ meV derived from tunneling experiment [34]. The in-plane anisotropy in both gap values, $s$ and $d$, is approximately the same, i.e., $\gamma_{ab}^{\Delta^d} = \Delta_{0,b}^{d}/\Delta_{0,a}^{d} = 1.09(1)$ and $\gamma_{ab}^{\Delta^s} = \Delta_{0,b}^{s}/\Delta_{0,a}^{s} = 1.15(6)$ (see

Table 1). Moreover, it is important to note that the $s$-wave gap along the $c$ direction $\Delta^s_{0,c} = 19.20(4)$ meV is of the same order of magnitude as the $d$-wave gaps in the $ab$ plane: $\Delta^s_{0,c} \simeq \Delta^d_{0,a} \simeq \Delta^d_{0,b} \approx 20$ meV.

In conclusion, we performed a systematic $\mu$SR study of the magnetic penetration depths $\lambda_a$, $\lambda_b$, and $\lambda_c$ on single crystals of $YBa_2Cu_4O_8$. In contrast to previous LFM experiments [19], our method is *bulk* sensitive and a direct probe of the penetration depth. The use of single crystals enables us to derive the magnetic penetration depth along the three principal crystallographic directions. Along the $a$ and $b$ directions, clear evidence is obtained that TGS is realized also in the chain containing compound $YBa_2Cu_4O_8$. While the in-plane penetration depth is anisotropic, exhibiting an inflection point at low temperatures in both $\lambda_a^{-2}$ and $\lambda_b^{-2}$ which is characteristic of TGS, the $c$-axis data provide clear evidence for an isotropic $s$-wave gap. From the data, it must be concluded that the in-plane superconducting gap consists of two components, namely $s + d$. The situation along the $c$-axis is different and supports $s$-wave only. This exceptional behavior has not been predicted by any theory, since the third dimension has mostly been neglected. Since $YBa_2Cu_4O_8$ differs structurally substantially from the previously investigated system $La_{2-x}Sr_xCuO_4$, where the in-plane penetration depth also shows $s+d$ wave superconductivity [14], the above findings cannot be attributed to specific structural features of the chain containing compound, but show that $s + d$ order parameters are generic, intrinsic, and common to all HTS. The results thus exclude theoretical approaches as, e.g., the "plain vanilla" mechanism which concentrates on the $CuO_2$ plane only. Besides the fact that t-J or 2D Hubbard models are not capable to yield the observed $s$-wave component, the role of the lattice played for superconductivity has to be reconsidered since the presence of an $s$-wave component naturally points to its importance.

**Acknowledgements** This work was partly performed at the Swiss Muon Source (S$\mu$S), Paul Scherrer Institute (PSI, Switzerland). The authors are grateful to A. Amato and R. Scheuermann for assistance during the $\mu$SR measurements. This work was supported by the Swiss National Science Foundation, the K. Alex Müller Foundation, and in part by the SCOPES grant No. IB7420-110784, the EU Project CoMePhS, and the NCCR program MaNEP.

## References

1. Suhl, H., Matthias, B.T., Walker, L.R.: Phys. Rev. Lett. **3**, 552 (1959)
2. Moskalenko, V.: Fiz. Metall. Metalloved. **8**, 503 (1959)
3. Kresin, V.Z.: J. Low Temp. Phys. **11**, 519 (1973)
4. Binnig, G., Baratoff, A., Hoenig, H.E., Bednorz, J.G.: Phys. Rev. Lett. **45**, 1352 (1980)
5. Iavarone, M., Karapetrov, G., Koshelev, A.E., Kwok, W.K., Crabtree, G.W., Hinks, D.G., Kang, W.N., Choi, E.-M., Kim, H.J., Kim, H.-J., Lee, S.I.: Phys. Rev. Lett. **89**, 187002 (2002)
6. Bussmann-Holder, A., Simon, A., Bishop, A.R.: Europhys. Lett. **75**, 308 (2006)
7. Müller, K.A.: Nature (London) **377**, 133 (1995)
8. Müller, K.A., Keller, H.: In: High-$T_c$ Superconductivity 1996: Ten Years after Discovery, pp. 7–29. Kluwer Academic, Dordrecht (1997)
9. Willemin, M., Rossel, C., Hofer, J., Keller, H., Ren, Z.F., Wang, J.H.: Phys. Rev. B **57**, 6137 (1998)
10. Limonov, M.F., Rykov, A.I., Tajima, S., Yamanaka, A.: Phys. Rev. Lett. **80**, 825 (1998)
11. Müller, K.A.: Phil. Mag. Lett. **82**, 279 (2002), and references therein
12. Deutscher, G.: Rev. Mod. Phys. **77**, 109 (2005)
13. Furrer, A.: In: Superconductivity in Complex Systems, pp. 171–204. Springer, Berlin (2005)
14. Khasanov, R., Shengelaya, A., Maisuradze, A., La Mattina, F., Bussmann-Holder, A., Keller, H., Müller, K.A.: Phys. Rev. Lett. **98**, 057007 (2007)
15. Bussmann-Holder, A., Khasanov, R., Shengelaya, A., Maisuradze, A., La Mattina, F., Keller, H., Müller, K.A.: Europhys. Lett. **77**, 27002 (2007)
16. Karpinski, J., Meijer, G.I., Schwer, H., Molinski, R., Kopnin, E., Conder, K., Angst, M., Jun, J., Kazakov, S., Wisniewski, A., Puzniak, R., Hofer, J., Alyoshin, V., Sin, A.: Supercond. Sci. Technol. **12**, R153 (1999)
17. Brandt, E.H.: Phys. Rev. B **37**, R2349 (1988)
18. Ager, C., Ogrin, F.Y., Lee, S.L., Aegerter, C.M., Romer, S., Keller, H., Savić, I.M., Lloyd, S.H., Johnson, S.J., Forgan, E.M., Riseman, T., Kealey, P.G., Tajima, S., Rykov, A.: Phys. Rev. B **62**, 3528 (2000)
19. Panagopoulos, C., Tallon, J.L., Xiang, T.: Phys. Rev. B **59**, R6635 (1999)
20. Khasanov, R., Kondo, T., Schmalian, J., Kazakov, S.M., Zhigadlo, N.D., Karpinski, J., Fretwell, H.M., Keller, H., Mesot, J., Kaminski, A.: cond-mat/0609385 (2006)
21. Mühlschlegel, B.: Z. Phys. **155**, 313 (1959)
22. Rammer, J.: Europhys. Lett. **5**, 77 (1988)
23. Xiang, T., Wheatley, J.M.: Phys. Rev. Lett. **77**, 4632 (1996)
24. Sun, A.G., Gajewski, D.A., Maple, M.B., Dynes, R.C.: Phys. Rev. Lett. **72**, 2267 (1994)
25. Li, Q., Tsay, Y.N., Suenaga, M., Klemm, R.A., Gu, G.D., Koshizuka, N.: Phys. Rev. Lett. **83**, 4160 (1999)
26. Kabanov, V.V., Demsar, J., Podobnik, B., Mihailovic, D.: Phys. Rev. B **59**, 1497 (1999)
27. Müller, K.A.: Inst. Phys. Conf. Ser. **181**, 3 (2004)
28. Klemm, R.A., Rieck, C.T., Scharnberg, K.: Phys. Rev. B **61**, 5913 (2000)
29. Lu, D.H., Feng, D.L., Armitage, N.P., Shen, K.M., Damascelli, A., Kim, C., Ronning, F., Shen, Z.-X., Bonn, D.A., Liang, R., Hardy, W.N., Rykov, A.I., Tajima, S.: Phys. Rev. Lett. **86**, 4370 (2001)
30. Smilde, H.J.H., Golubov, A.A., Rijnders, A.G., Dekkers, J.M., Harkema, S., Blank, D.H.A., Rogalla, H., Hilgenkamp, H.: Phys. Rev. Lett. **95**, 257001 (2005)
31. Smilde, A.H.J.H., Verwijs, C.J.M., Rijnders, G., Blank, D.H.A., Rogalla, H., Kirtley, J.R., Tsuei, C.C., Hilgenkamp, H.: arXiv: cond-mat/0606248v2 (2006)
32. Friedl, B., Thomsen, C., Cardona, M.: Phys. Rev. Lett. **65**, 915 (1990)
33. Basov, D.N., Liang, R., Bonn, D.A., Hardy, W.N., Dabrowski, B., Quijada, M., Tanner, D.B., Rice, J.P., Ginsberg, D.M., Timusk, T.: Phys. Rev. Lett. **74**, 598 (1995)
34. Karpinski, J., Schwer, H., Conder, K., Lohle, J., Molinski, R., Morawski, A., Rossel, Ch., Zech, D., Hofer, J.: In: Klamut, J., et al. (eds.) Recent Developments in High Temperature Superconductivity. Lecture Notes in Physics, pp. 83–102. Springer, New York (1996)